

Study of a narrowband reflection filter with multi-channels

Hongfei Jiao (焦宏飞)^{1,2*}, Tao Ding (丁涛)¹, Xinbin Cheng (程鑫彬)¹,
Bin Ma (马彬)^{1,2}, Pengfei He (贺鹏飞)², and Yonggang Wu (吴永刚)¹

¹Institute of Precision Optical Engineering, Department of Physics, Tongji University, Shanghai 200092, China

²School of Aerospace Engineering and Applied Mechanics, Tongji University, Shanghai 200092, China

*E-mail: jiaohf@tongji.edu.cn

Received March 3, 2010

Reflection filters have various applications in optical communication and other systems. In this letter, we propose a narrowband high-reflection filter composed of dielectric and metallic layers, in which an optimized filter combined with an admittance-matching layer with broad stop band is achieved. The structure can be expressed as Sub | (HL)¹³H2L(HL)³13Cr0.84H | air, with full-width at half-maximum (FWHM) bandwidth of 2.5 nm. Based on this structure, reflection filters with multi-peaks are presented, and the law of distribution of peak positions is drawn.

OCIS codes: 310.6860, 230.7408, 220.0220.

doi: 10.3788/COL20100811.1102.

Interference filters have a huge prospect of being applied in the fields of optical communication, space engineering, industrial detection^[1–6], and so on. Filters with multiple channels are especially fascinating in a dense wavelength division multiplexing (DWDM) system; such filters are called transmittance filters. Likewise, reflection filters also have various applications in fields such as special photography and communication systems^[7,8]. Considerable research has been done on the design and fabrication of reflection filter. For instance, Thelen proposed an all-dielectric minus filter^[9], while Wang *et al.* presented a multi-peak reflection filter using guided resonant gratings^[10]. Sheng *et al.* designed a reflection filter by alternately superimposing metal and dielectric layers^[11], and Robin *et al.* produced a reflectance filter with a metal/dielectric/metal structure^[7,12]. However, these filters are difficult to fabricate because of their complicated non-period structures. Sun *et al.* recently proposed a new structure by adding one metal layer to a period dielectric film stack, which is easier to fabricate^[13,14].

In this letter, a new structure based on Sun's model is proposed; it has improved spectral characteristics through the addition of a suitable matching layer. In addition, further investigation on multi-channel and integrated reflection filters is carried out.

We chose the structure Sub | (HL)⁷H2L(HL)³ α Cr | air, which was proposed by Sun *et al.*^[13], as the starting structure for optimization. In the structure, Sub means substrate, H represents a dielectric layer (TiO₂) with assumed high refractive index value of 2.16; L is a dielectric layer (SiO₂) with assumed low refractive index value of 1.46; the optical thickness of the corresponding layer is equal to one quarter of the desired central wavelength. We assume that the refractive index for the substrate is 1.52. The refractive indices of Cr are adopted from the handbook of Palik^[15] and are described in Table 1. The physical thickness of the metal Cr layer is represented by α . The designed wavelength is 700 nm.

The structure (HL)^{*m*}H2L(HL)^{*n*} is similar to the Fabry-Perot (F-P) mirror, which we call quasi-F-P in this letter. Assuming (HL)^{*m*}H and (HL)^{*n*} to be the first and

the second mirrors, respectively, they play different roles in the filter; this has been discussed in part in previous studies^[14,16]. Figure 1(a) shows the reflectance spectra, wherein *n* is equal to 3 with different *m* values of 6, 7, 8, and 9. Figure 1(b) shows the case of fixed *m* = 6 with varying *n* values of 2, 3, 4, and 5. Figure 1(c) shows the case of fixed *m* = 9 with varying *n* values of 2, 3, 4, and 5. The insets are enlarged drawing of the peaks. The result shows that there is a need to increase the value of *m* in order to improve the height of the peaks. It is also shown that the bandwidth will become narrower when the value of *n* is increased. However, the value of *n* cannot be too big; it should be less than the value of *m* to maintain a sufficiently high reflectance at the central wavelength. Moreover, with increasing value of *n*, the curve distributed around the central wavelength will become more unstable, leading to a poor cut-off band. Thus, there is a need to choose a suitable parameter to achieve the required results.

Figure 2 shows the reflectance and absorptance spectra of the filter: Sub | (HL)⁷H2L(HL)³ α Cr | air; the inset is an enlarged drawing of the peaks. It can be seen that the reflectance curve of the stop band becomes flatter as the thickness of the Cr layer increases. However, the height of the reflectance at the central wavelength remains almost unchang. It can also be seen that the absorptance at the central wavelength is kept at the minimum throughout, while the other curves around the central wavelength become flatter. From these observations, it can be said that there is a need to find the suitable thickness of the Cr layer that will enable the filter to have a better

Table 1. Refractive Index *n* and Extinction Coefficient *k* of Cr Thin Films

Wavelength (nm)	490.1	512.3	532.1	558.5	582.1
<i>n</i>	2.49	2.75	2.98	3.18	3.34
<i>k</i>	4.44	4.46	4.45	4.41	4.38
Wavelength (nm)	610.8	700.5	815.7	826.6	849.2
<i>n</i>	3.48	3.84	4.23	4.27	4.31
<i>k</i>	4.36	4.37	4.34	4.33	4.32

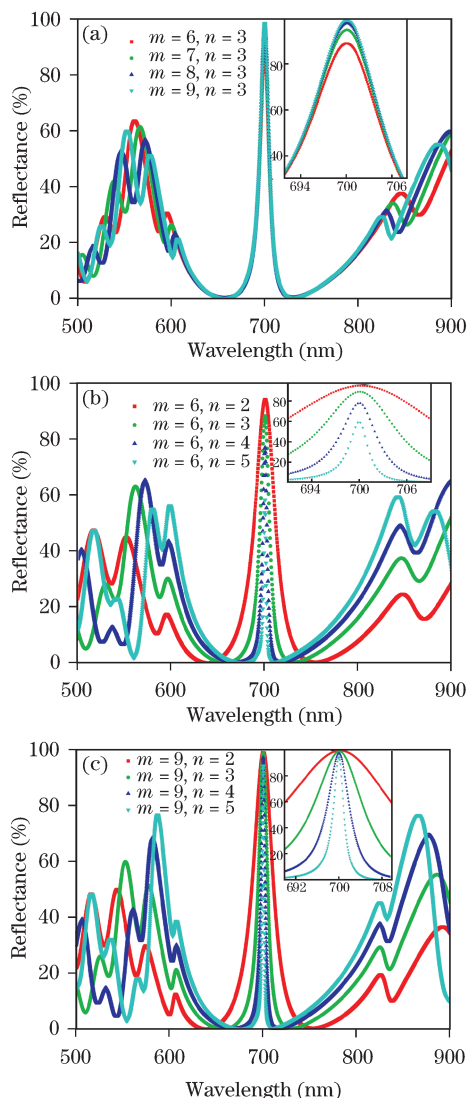


Fig. 1. Reflectance spectra of filters: Sub | (HL)^mH2L(HL)ⁿ αCr | air, where α = 3 nm; design wavelength 700 nm. Inset is the enlarged drawing of peaks. (a) n = 3, m equals 6, 7, 8, and 9, respectively; (b) m = 6, n equals 2, 3, 4, and 5, respectively; (c) m = 9, n equals 2, 3, 4, and 5, respectively.

cut-off characteristic and a broader stop band.

The equivalent admittance Y of the film stack can be expressed as

$$Y = y_{re} + iy_{im}, \quad (1)$$

where y_{re} is the real part of the admittance, and y_{im} is the imaginary part of the admittance. Meanwhile, the admittance of the incidence medium is N_0 (in this letter, the incidence medium is air; thus, $N_0 = 1$), and amplitude reflectance r and reflectance R can be respectively expressed as

$$r = \frac{N_0 - Y}{N_0 + Y} = \frac{(N_0 - y_{re}) - iy_{im}}{(N_0 + y_{re}) + iy_{im}}, \quad (2)$$

$$R = \frac{(N_0 - y_{re})^2 + y_{im}^2}{(N_0 + y_{re})^2 + y_{im}^2}. \quad (3)$$

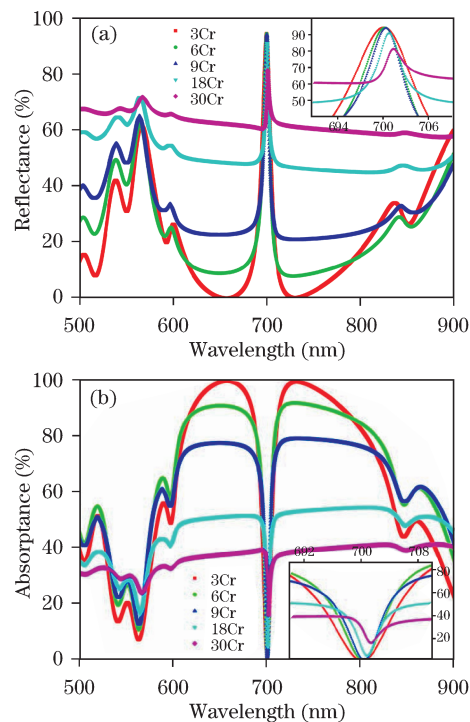


Fig. 2. (a) Reflectance and (b) absorbance spectral of filters: Sub | (HL)⁷H2L(HL)³αCr | air, design wavelength 700 nm. Inset is the magnified peaks. The different thickness of Cr almost does not have an impact on the maximum (minimum) peaks of reflectance (absorbance) spectra, and the curve turns smooth with the increasing thickness of the Cr layer.

From Eq. (3), it can be seen that for the filter to have a better cut-off, that is, if we want the reflectance outside the central wavelength to be 0, the following equation should be satisfied:

$$\begin{cases} y_{re} = N_0 = 1 \\ y_{im} = 0 \end{cases}. \quad (4)$$

To satisfy Eq. (4), an admittance-matching layer should be added to the filter, through which the admittance of the whole film stack will match the incidence medium. Once completed, a filter with almost 100% reflectance at the central wavelength and zero reflectance around the central wavelength can be realized.

Based on the previously discussed results, to achieve a sufficiently high reflectance at the central wavelength and a better cut-off band, we chose the following parameters: $m = 13$, $n = 3$, and $\alpha = 13$ nm. Figures 3(a) and (b) show the distributions of equivalent admittance versus wavelength. The structure of Fig. 3(a) is Sub | (HL)¹³H2L(HL)³13Cr | air; there is no matching layer in this structure, although y_{im} is close to 0 and y_{re} has a huge deviation from 1. Meanwhile, the structure of Fig. 3(b) is Sub | (HL)¹³H2L(HL)³13Cr0.84H | air, to which a matching layer has been added using TiO₂ with 0.84 quarter optical thickness; y_{re} is close to 1, while y_{im} is close to 0. Figure 3(c) shows the comparison of the reflectance between the two structures, where the cut-off depth decreased from 40% to 0% after adding the admittance-matching layer.

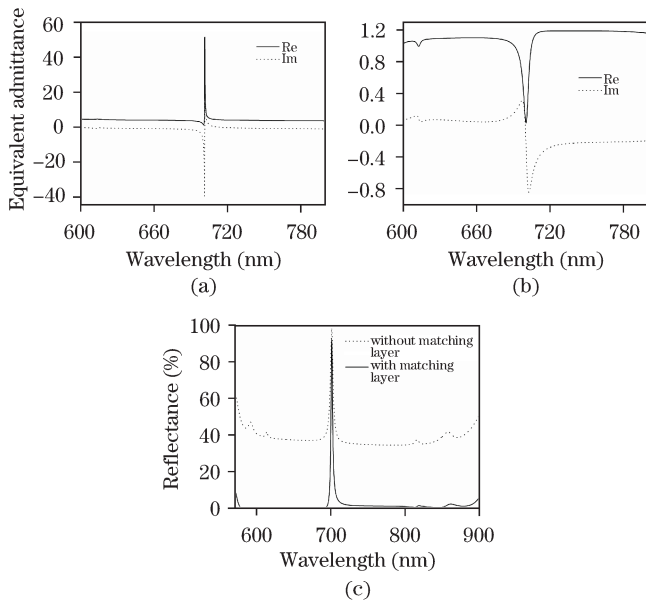


Fig. 3. Equivalent admittance versus wavelength for the structures (a) Sub | (HL)¹³H2L(HL)³13Cr | air and (b) Sub | (HL)¹³H2L(HL)³13Cr0.84H | air, where the real and imaginary parts are shown by solid and dotted lines, respectively. (c) Reflectance spectra comparison of two structures; design wavelength 700 nm.

As discussed above, the optimal parameters are $m = 13$, $n = 3$, and $\alpha = 13$ nm; the matching layer is 0.84H. As shown in Fig. 3, the reflectance at the central wavelength is higher than 90%, full-width at half-maximum (FWHM) bandwidth is 2.5 nm, and the stop band is broader than 300 nm.

Based on our previous study about one-dimensional (1D) multi-channel photonic crystal^[3], some characteristics of multi-peak reflection filters can be drawn using a similar method. By knowing the function of every part in the previously proposed reflection filter structure, many multi-channel reflection filters can be composed. In this research, we study a new similar structure composed of three channels: Sub | (HL)¹³(HL)² p H(LH)² β L(HL)² q H(LH)²L13Cr0.84H | air, where p , β , and q are real numbers and β should not be lower than 4. There are three resonances, namely, p H, β L, and q H, which correspond to three peaks, respectively, arranged from left to right. The rule of position distribution is discussed as follows.

A simple sample (the values of p and q are close to 2 and $\beta = 4$) is discussed here for the case of β being an even integer, and a detailed research will be carried out in a later study.

Firstly, if β is fixed; p and q are the variables; $p+q < \beta$, then all three peaks will move toward the short wavelengths and there would be no peak at the central wavelength. The position of the peaks will remain unchanged even if the values of p and q are swapped, which is shown in Fig. 4(a).

Secondly, if β is fixed; p and q are variables; $p+q > \beta$, then all three peaks will move toward the long wavelengths and there would be no peak at the central wavelength. The position of the peaks will remain unchanged even if the values of p and q are swapped, which is shown in Fig. 4(b).

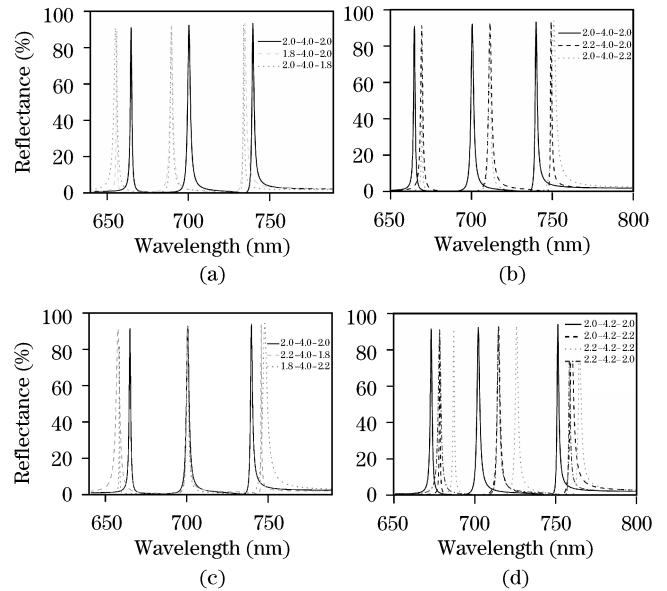


Fig. 4. Reflectance spectra of filters with three resonances Sub | (HL)¹³(HL)² p H(LH)² β L(HL)² q H(LH)²L13Cr0.84H | air; design wavelength 700 nm.

Thirdly, if β is fixed, p and q are variables; $p+q = \beta$, then the position of the middle peak will remain unchanged, while the the left and right peak positions will move to the short and long wavelengths, respectively. The position of the peaks will remain unchanged even if the values of p and q are swapped, as shown in Fig. 4(c).

Fourthly, if $(p+q)$ is fixed, β is the variable, and $\beta \in ([\beta], [\beta] + 1)$, then the position of the middle peak will move to the long wavelength along with the increase of β and *vice versa*. The positions of the peaks will remain unchanged even if the values of p and q are swapped (Fig. 4(d)).

From Fig. 4, it can also be seen that apart from the change of peak positions, the peak bandwidth will also turn narrower when p or q changes to a lower value compared with the origin one.

Fifthly, we take a special structure for study: Sub | (HL)¹³(HL)²2H(LH)² β L(HL)²2H(LH)²L13Cr0.84H | air,

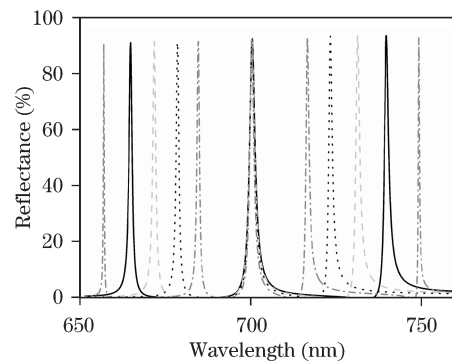


Fig. 5. Reflectance spectra of filters Sub | (HL)¹³(HL)²2H(LH)² β L(HL)²2H(LH)²L13Cr0.84H | air, where β equals 4 (solid), 8 (dash), 16 (dot), and 32 (dash dot), respectively; design wavelength 700 nm. With β doubled, the central peak remains at 700 nm, while the other peaks distributed around the central peak almost equidistantly move to the central one.

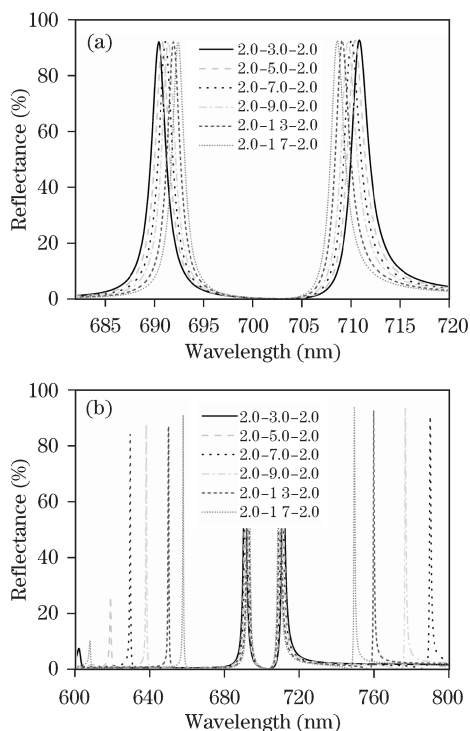


Fig. 6. Reflectance spectra of filters Sub | (HL)¹³ (HL)² 2H (LH)² β L (HL)² 2H (LH)² L 13Cr 0.84H | air, where β equals 3 (solid), 5 (dash), 7 (dot), 9 (dash dot), 13 (short dash), and 17 (short dot), respectively; design wavelength 700 nm.

where $p = q = 2$ and β equals 4, 8, 16, and 32, respectively. As shown in Fig. 5, the position of the central peak remains unchanged even if the value of β is doubled, while both side peaks move toward the central wavelength equidistantly. When β is big enough, the secondary interference peaks will appear.

Now consider the case of β being an odd integer. Take structure Sub | (HL)¹³ (HL)² 2H (LH)² β L (HL)² 2H (LH)² L 13Cr 0.84H | air as an example, where $p = q = 2$ and β is the variable equaling 3, 5, 7, 9, 13, and 17, respectively. As shown in Fig. 6(a), there are only two peaks near the central wavelength without reflectance peak at the central wavelength (700 nm). The left and right peaks move gradually toward the central wavelength by increasing the value of β ; at the same time, the secondary interference peaks appear. Moreover, as β becomes bigger, the positions of the secondary interference peaks become nearer the central wavelength, which can be seen in Fig. 6(b).

This means that with the structure Sub | (HL)¹³ (HL)² p H (LH)² β L (HL)² q H (LH)² L 13Cr 0.84H | air, when β equals an even integer, there will be reflectance peak in the central wavelength. Meanwhile, when β equals an odd integer, there will be no peak at

the central wavelength. At the same time, when p and q are fixed, the position will move toward the central wavelength along with the increase of β .

In conclusion, a narrowband high-reflection filter composed of dielectric and metal is proposed. By studying the function of metal and dielectric layers, a modified filter with admittance-matching layer having the structure Sub | (HL)¹³ H₂L (HL)³ 13Cr 0.84H | air is achieved. The new structure has FWHM bandwidth of 2.5 nm with a broad stop band over 300 nm. Based on this structure, a reflection filter with multi-peaks is presented and the law of distribution of peak positions is drawn, resulting in various applications in optical communication and other systems.

This work was supported partially by the National Natural Science Foundation of China (No. 10175049) and the National "863" Program of China.

References

1. S. Wang, L. Wang, Y. Wu, Z. Wang, D. Liu, B. Lin, X. Chen, and W. Lu, *Acta Opt. Sin.* (in Chinese) **26**, 746 (2006).
2. Y. Wu, G. Tian, Z. Wang, and X. Lin, "Design and modification of adjustable double channel filter" (in Chinese) Chinese patent 200410053814.8 (March 2, 2005).
3. H. Jiao, Y. Wu, G. Tian, S. Wang, H. Cao, L. Zhang, and L. Fu, *Appl. Opt.* **46**, 867 (2007).
4. G. Tian, Y. Wu, Z. Wang, X. Lin, Y. Wang, T. Qi, and L. Chen, *Acta Opt. Sin.* (in Chinese) **25**, 661 (2005).
5. Z. Wang, Y. Wu, T. Sang, Z. Wang, D. Peng, H. Jiao, N. Chen, and H. Cao, *Acta Opt. Sin.* (in Chinese) **29**, 849 (2009).
6. Z. Wang, T. Sang, L. Wang, H. Jiao, Y. Wu, J. Zhu, L. Chen, S.-W. Wang, X. Chen, and W. Lu, *Appl. Opt.* **47**, C1 (2008).
7. R. Gamble and P. H. Lissberger, *Appl. Opt.* **28**, 2838 (1989).
8. J.-S. Sheng and J.-T. Lue, *Appl. Opt.* **31**, 6117 (1992).
9. A. Thelen, *J. Opt. Soc. Am.* **61**, 365 (1971).
10. Z. Wang, T. Sang, J. Zhu, L. Wang, Y. Wu, and L. Chen, *Appl. Phys. Lett.* **89**, 241119 (2006).
11. J.-S. Sheng, J.-T. Lue, and J.-H. Tyan, *Appl. Opt.* **30**, 1746 (1991).
12. M. Tan, Y. Lin, and D. Zhao, *Appl. Opt.* **36**, 827 (1997).
13. X. Sun, P. Gu, W. Shen, X. Liu, Y. Wang, and Y. Zhang, *Appl. Opt.* **46**, 2899 (2007).
14. W. Shen, X. Sun, Y. Zhang, Z. Luo, X. Liu, and P. Gu, *Opt. Commun.* **282**, 242 (2009).
15. E. D. Palik, (ed.) *Handbook of Optical Constants of Solids* (Academic Press, San Diego, 1991).
16. Y. Wu, H. Jiao, D. Peng, Z. Wang, L. Fu, G. Lu, N. Chen, and L. Ling, *Appl. Opt.* **47**, 5370 (2008).